Nanomaterials

Cerium Phosphate Nanotubes: Synthesis, Valence State, and Optical Properties**

Chengchun Tang, Yoshio Bando, Dmitri Golberg, and Renzhi Ma*

Metal phosphates are widely utilized in nonlinear optical materials, phosphors, sensors, heat-resistant, and biocompatible materials. A particular emphasis has been placed on the study of rare-earth or rare-earth-doped phosphate materials for applications in photonic devices.[1] This interest is primarily attributed to the position of the 4f electrons, which are well shielded from the effects of the neighboring ions. Such shielding leads to discrete and well-defined energy level schemes, as well as to rather weak coupling between the electronic and vibrational wave functions. The specific luminescence with a characteristic long lifetime originates from the f–f emissions. However, at present, the progress with regard to new luminescent materials is chiefly focussed on short emission wavelengths, which are useful for imaging, lithography, and optical data recording.[2] The rare-earth ions Ce^{3+} and Sm^{2+} exhibit a 5d–4f emission with a larger absorption in the UV region and a shorter luminescence lifetime due to allowed electric dipole transitions; thus, they display excellent properties for applications in these fields.[3] On the other hand, although the doping of transparent Ce^{4+} ions in luminescence materials has been prohibited due to the competitive absorption in UV region, some Ce^{3+}/Ce^{4+} hybrid systems in glass hosts exhibit a strong blue emission, which possibly results from electron transfer from a donor level to the neighboring Ce^{4+} ions, consequently forming excited states of Ce^{3+} ions.[4] Taking into account the strong UV absorption of Ce^{4+} ions, such hybrid structures are good candidates for materials that display blue emission with high absorption and fast emissive rates.[5]

One-dimensional nanomaterials, that is, nanotubes made of, for example, C, BN, WS_2, VO_x, TiO_2, and InP[6] have been synthesized and display novel properties that are frequently different from those of the bulk forms. However, the synthesis and emission behaviour of nanotube-like hybrid materials containing Ce^{4+}/Ce^{3+} ions has received much less attention.

Herein, we report on a reproducible and controllable route for the production of cerium phosphate nanotubes, the first rare-earth phosphate nanotubes. Tetravalent cerium phosphate (CeP, $Ce(HPO_4)_2{\cdot}nH_2O$) nanotubes were first synthesized after improving the traditional synthetic route toward a CeP fiber.[7] Subsequent annealing of the as-synthesized nanotubes led to a mixture of valence states, and the desired Ce^{3+}/Ce^{4+} hybrid phosphate nanotubes were obtained for the first time. The nanotubes display novel optical properties; that is, the Ce^{4+} ions effectively absorb the UV light, whereas the Ce^{3+} ions exhibit strong emission in the blue region of a photoluminescence spectrum.

It has been reported that a high PO_4/Ce ratio (20:1–120:1) in the initial solution and a high reaction temperature (up to 95 °C) are needed to form a CeP fiber.[7,8] In this study, we have increased the PO_4/Ce ratio to 300:1 and increased the reaction temperature to above 95 °C. Figures 1 a–d show the scanning electron microscope (SEM) images of a CeP material synthesized at 70, 90, and 105 °C, respectively. A fibrous structure can be found for all the samples examined, although an amorphous phase may exist in a lower temperature product (ca. 50–80 °C), and some microcrystalline particles are visible in a higher temperature product (> 95 °C). X-ray diffraction (XRD) measurements indicate that the CeP material displays different crystalline structures, depending on the reaction temperature (Figure 1 e). The XRD patterns of a CeP sample synthesized at temperatures lower than 70 °C show broad peaks and a peak at about 7.8°

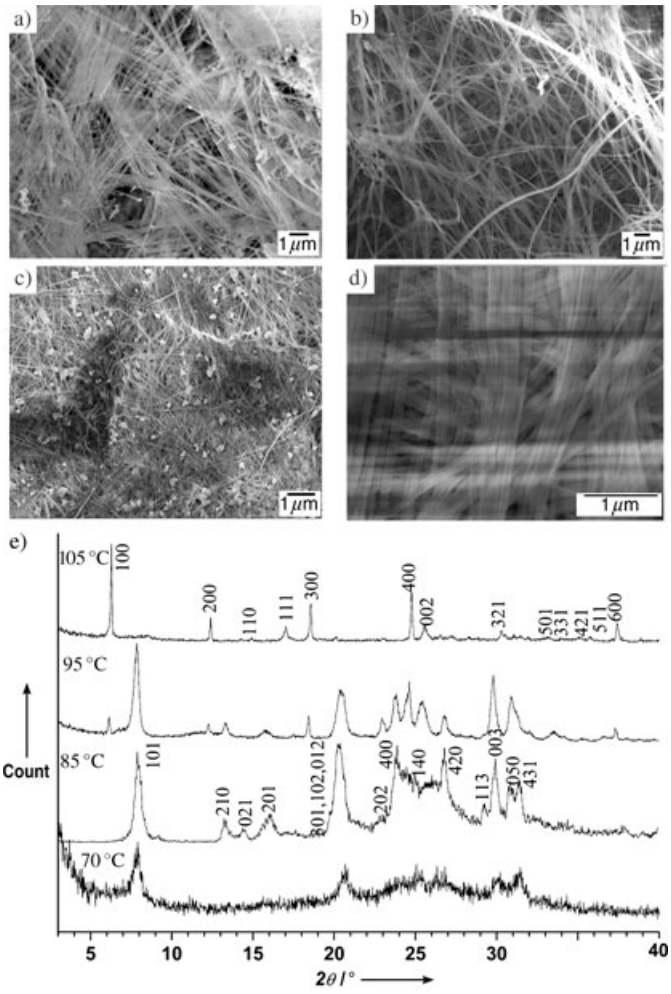

Figure 1. SEM images of a CeP nanomaterial synthesized at 70 (a), 90 (b), and 105 °C (c, d). e) The representative XRD patterns recorded for the products synthesized at different temperatures.

[*] Dr. C. Tang, Prof. Y. Bando, Dr. D. Golberg, Dr. R. Ma
Advanced Materials Laboratory
National Institute for Materials Science (NIMS)
1-1 Namiki, Tsukuba, Ibaraki 305-0044 (Japan)
Fax: (+81) 29-851-6280
E-mail: tang.chengchun@nims.go.jp

[**] We thank Y. Uemura and R. Xie for their help in the measurement of the absorption spectra.

  DOI: 10.1002/ange.200461171

(2θ), $d = 1.12$ nm, indicating a layered structure. Thermogravimetric analyses indicate that the water content in CeP varies from $n = \approx 2$ to ≈ 3, depending on the temperature at which the synthesis was carried out. The comparison of the d spacing and the relative intensities measured for the XRD patterns with those of a CeP ($Ce(HPO_4)_2 \cdot H_2O$) fiber,[8] reveal a fairly good agreement, except for a slightly expanded layer-to-layer distance ($d = 1.10$ nm, the difference may result from the variations in the water content in CeP). Though the detailed crystal structure is still unknown, the present pattern can be readily indexed to an orthorhombic structure ($a = 1.494$, $b = 1.436$, $c = 0.906$ nm). On increasing the temperature, the CeP nanomaterial gradually changes its morphology (Figure 1). An XRD pattern of CeP synthesized at 105 °C can be indexed to a hexagonal structure with the lattice parameters ($a = 1.668$, $c = 0.678$ nm). Thermogravimetric analysis suggested that the formula of the novel phase was $Ce(HPO_4)_2 \cdot H_2O$. The two phases coexist from 90 to 100 °C, but the orthorhombic phase is rarely observed when the synthesis temperature is higher than 100 °C.

An important consequence of the temperature-dependent transformation is the appearance of a nanotube-like morphology. The CeP material synthesized below 90 °C usually comprises solid fibers with diameters ranging from several tens of nanometers up to about 500 nm (Figure 1a and b). However, the diameters of the nanofibers of the CeP material synthesized at 105 °C are smaller and more unified in size (20 to 100 nm; see the transmission electron microscope (TEM) image in Figure 2a). The nanotubes become the dominant morphology, though some nanofibers with a diameter of several tens of nanometers can be occasionally observed. Figure 2b shows the magnified image of an individual nanotube. The nanotubes are usually open at their tips. The tubular morphology was verified by tilting the sample in the transmission electron microscope, while recording the corresponding selected-area electron diffraction (SAED) pattern (inset, Figure 2b). The pattern recorded along the [110] zone axis clearly exhibits the "zigzag"-type chirality of a tubular shell.[9] Although the CeP nanotubes were unstable under irradiation with an electron beam, we were able to obtain high-resolution TEM images that confirmed the nanotube-like morphology (Figure 2c).

X-ray photoelectron spectroscopy (XPS) can usually provide clear information about the valence state of Ce; however, in this study it was not applied because minor amorphous and/or microcrystal impurities exist in the products. Therefore, the chemical valence of the cerium ions within an individual CeP nanotube was determined by using a parallel electron energy loss spectrometer (EELS), taking into consideration that the occupancy of the 4f shell of light lanthanides is sensitive to the ratio of the $3d_{3/2} \rightarrow 4f_{5/2}$ (M_4) to $3d_{5/2} \rightarrow 4f_{7/2}$ (M_5) peak areas.[10] The EEL spectrum of the CeP nanotubes (Figure 2d) contains the features consistent with the multiplet structure of the $3d^9 4f^2$ final states (M_5 at ca. 884 eV and M_4 at ca. 901 eV).[11] The extra peaks, about 7 eV higher in energy than the M_4 and M_5 lines, respectively, are clearly detected, indicating the existence of Ce^{4+}.[12] The fitted M_4/M_5 ratio for the EEL spectrum is about 1.20:1; thus, in accord with the reference M_4/M_5 values of 0.78:1 for trivalent cerium orthophosphate and 1.1:1 for CeO_2,[10] the Ce^{4+} states should be present, although there has been much debate concerning the existence of pure Ce^{4+}.

The temperature-dependent stability of Ce valences in CeP nanotubes was analyzed by using a temperature-controlled annealing procedure under a reduced atmosphere. Such an atmosphere can maintain the one-dimensional morphology up to about 900 °C (Figure 3a), although the formation of glass-phase particles is visible in the SEM images (dark contrast areas within the fibers). The TEM images indicate that no nanotubes were present in the sample heat-treated at 900 °C. The initial nanotubes are thus completely transformed into solid fibers. Figure 3b displays a high-resolution TEM image of a polycrystalline nanowire with diameters similar to those of the starting nanotubes. However,

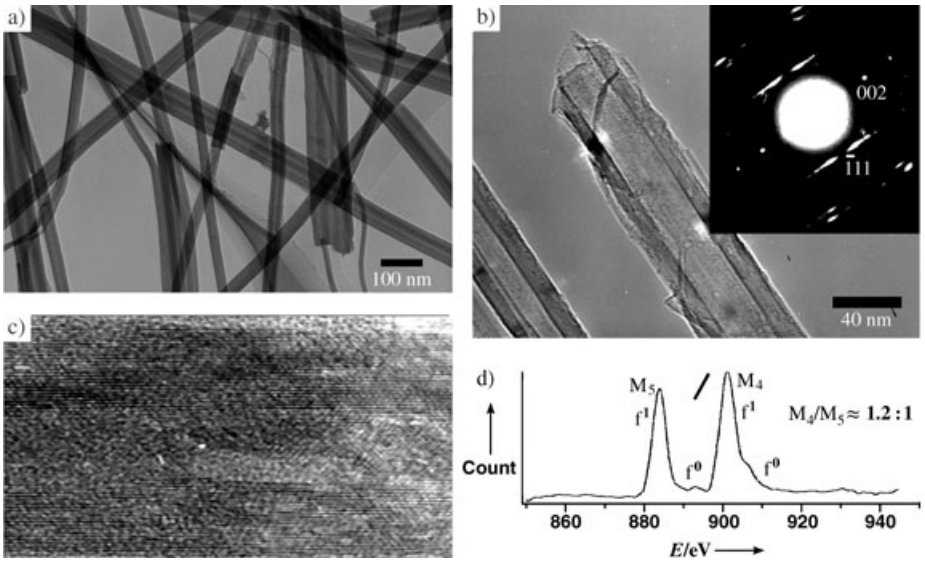

Figure 2. CeP nanotubes synthesized at 105 °C: a) Low-magnification TEM image revealing a tube-like morphology; b) TEM image of a nanotube and its corresponding SAED pattern; c) high-resolution TEM image of a nanotube with a diameter of about 20 nm; d) EEL spectrum displaying the characteristics for a tetravalent cerium ion.

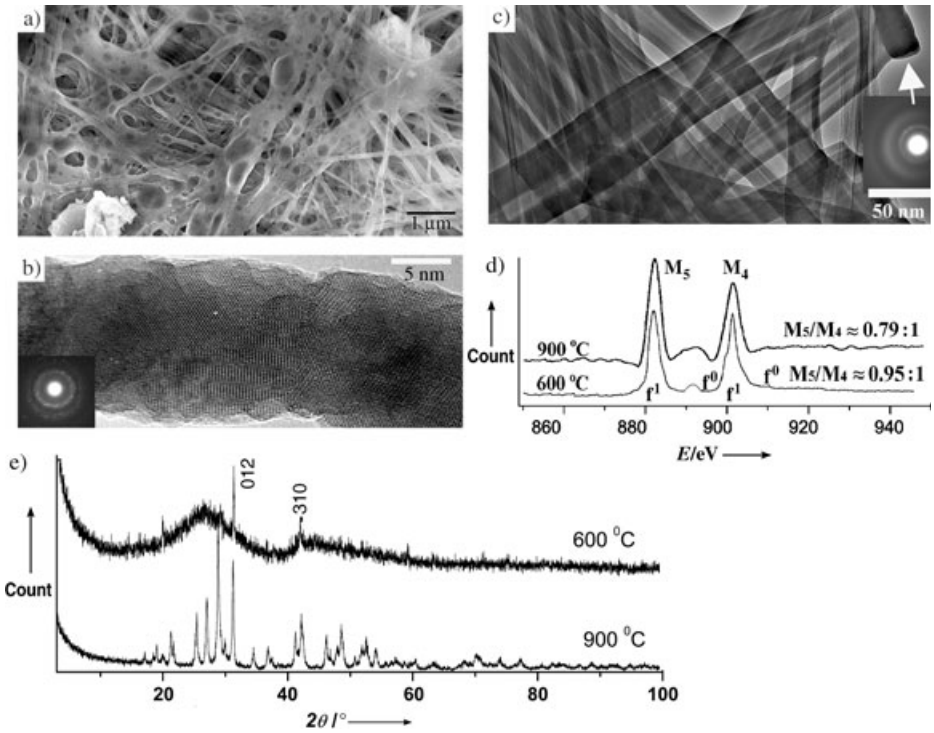

Figure 3. a) SEM image of CeP nanowires synthesized by annealing CeP nanotubes at 900 °C, b) the corresponding high-resolution TEM image; the inset in b) is the SAED pattern recorded for an individual nanowire; c) TEM image of CeP nanotubes annealed at 600 °C; d) EEL spectra, and e) XRD patterns for the annealed samples.

the nanotubes represent a dominant morphology in the CeP products prepared at a relatively low temperature. The CeP nanotubes post-treated at 600 °C are shown in Figure 3c; the SAED pattern taken from the arrowed tip area clearly indicates a glass-like structure at the tip (inset).

The EEL spectra recorded for an individual nanotube (600 °C) and a nanowire (900 °C) are shown in Figure 3d. The measured M_4/M_5 ratio decreases from about 0.95:1 (600 °C) to about 0.79:1 (900 °C). Given that the ratio of about 0.79:1 is in a good agreement with the previously reported value for cerium(III) orthophosphate,[10] we assume that the CeP material produced during the heat treatment at 900 °C mainly contains trivalent cerium. By assuming a linear interpolation between the M_4/M_5 values for Ce^{4+} (1.20:1) and Ce^{3+} (0.79:1), a nominal valence of +3.34 was calculated for the cerium in CeP heated at 600 °C.

The XRD pattern recorded for CeP nanowires (Figure 3e) can be indexed to a monoclinic structure for which the peak positions and intensities are similar to those of trivalent monazite $CePO_4$ (JCPDS 32-0199). Analysis of the patterns obtained from CeP nanotubes post-treated at 600 °C seems to indicate that the trivalent phase is also present here, but there are only traces of it in an amorphous matrix.

Figure 4a displays the UV/Vis spectra of the CeP nanotubes and their post-treated products. Tetravalent CeP nanotubes that have not been heat-treated can absorb UV light, almost completely, with the cutoff wavelength of about 450 nm. The cutoff wavelength shifts to about 420 nm, when the CeP nanotubes are treated at 300 °C. The nonlinear spectrum with an absorption extension of 300–450 nm is caused by the Ce^{4+} ions, since their d-electron exited states exhibit strong electron–phonon coupling.[13] It is noteworthy that the absorption peaks attributed to the f–d electron transitions of Ce^{3+} (200–320 nm), can be observed in the samples heat-treated at a temperature higher than 300 °C. The absorption spectrum of a sample annealed at 600 °C consists of two overlapping patterns originating from Ce^{4+} bands (cutoff wavelength ca. 420 nm) and Ce^{3+} lines (visible absorptions at 210 and 235 nm). The absorption spectrum of CeP nanowires produced by heat treatment at 900 °C contains the characteristic peaks of Ce^{3+} with maxima at 208, 216, 227, 261, and 275 nm within an f–d transition absorption band. These peaks correspond to the theoretical values (203–276 nm) of Ce^{3+} f–d transitions from a $4f^1$ ground state to the five $5d^1$ levels split within a monoclinic crystal field.[14] The absorption characteristics are in good agreement with the mixed-valence state mentioned above.

Figure 4b displays the photoluminescence (PL) spectra. No luminescence was

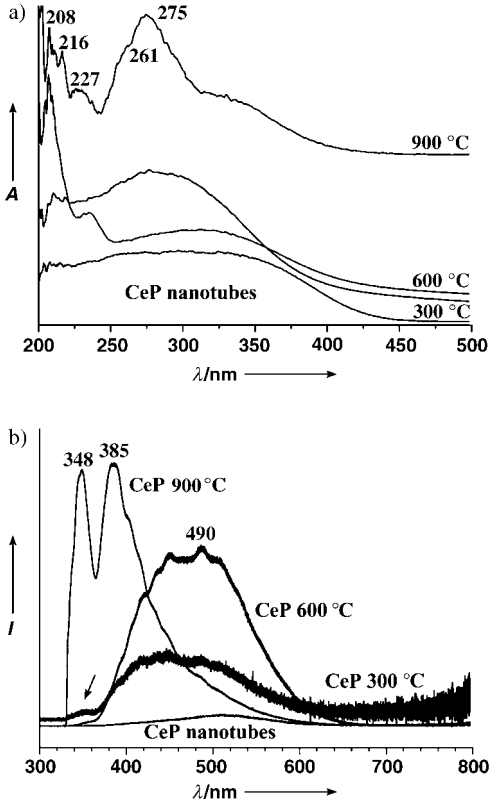

Figure 4. Absorption (a) and photoluminescence (b) spectra of CeP nanotubes and their products post-heat-treated at 300, 600, and 900 °C.

observed for the as-synthesized CeP nanotubes due to the absence of Ce^{3+}. The pure trivalent CeP nanowires exhibit strong UV luminescence; the two sharp peaks are centered at about 348 nm and about 385 nm with a full-width at half maximum (FWHM) of about 12 nm and about 30 nm, respectively. The double-peak luminescence corresponds to the direct emission from the $^2D(5d^1)$ state to the two split $4f^1$ ground states of $^2F_{5/2}$ and $^2F_{7/2}$ caused by spin-orbit coupling. The small FWHM values also imply that the exited state of Ce^{3+} is scarcely affected by the charge transfer transitions from the host ligands. In contrast to pure Ce^{3+} nanowires and Ce^{4+} nanotubes, the PL spectra of the Ce^{3+}/Ce^{4+} hybrid CeP nanotubes exhibit a strong blue luminescence. A broad and prominent blue emission at about 490 nm is visible for the $Ce^{+3.34}P$ nanotubes (heated at 600 °C; Figure 4b). Such a broad, blue emission for Ce^{3+} ions has been observed and attributed to a charge transfer.[4,15] The charge transfer between Ce^{4+} electron donation centers and Ce^{3+} luminescence centers in the present nanotubes may occur due to the electron–photon interaction. It has been reported that the 4f–5d bands of Ce^{3+} and the charge-transfer transition bands of Ce^{4+} ions appear in the same wavelength range and overlap.[16] Therefore, Ce^{4+} bands form the exited state and cause the blue emission. We also noticed that the intensity of the blue emission depends on the concentration of Ce^{3+} in a Ce^{4+} phosphate host. The hybrid CeP nanotubes heat-treated at 300 °C exhibit a weak blue emission. The direct emission of Ce^{3+} ions can be observed as an additional broad peak between 330 and 380 nm (see arrow in Figure 4b).

In summary, the first rare-earth metal phosphate nanotubes made of CeP have been synthesized by careful control of the composition of the reactants and the reaction temperature. Under post-heat treatments in a reduced atmosphere, the tubular morphology was maintained up to about 900 °C. Further increase in the temperature results in the formation of nanowires, and leads to valence change from +4 to +3 for the cerium ion. Strong blue and UV luminescence was observed for the Ce^{3+}/Ce^{4+} hybrid nanotubes and pure Ce^{3+} nanowires, respectively. Taking into account the short emission lifetime (a few ns) of Ce^{3+}, CeP one-dimensional nanostructures and, in particular, valence-hybrid nanotubes developed in the present work are promising candidates for light-emission-diode lamps, electroluminescence devices, non-mercury-fluorescent lamps, and plasma display panels.

Experimental Section

CeP nanotubes were prepared according to the procedure reported by Alberti et al,[7,8] though a higher reaction temperature range and reactant PO_4/Ce concentration ratio were used in the present work. The apparatus utilized was similar to that employed by Ali et al[17] to prepare phosphate salts. In our experiments, a 6 M aqueous phosphoric acid solution was first heated to a temperature ranging from 50 to 110 °C, and stirred for 4 h to form a condensed linear polyphosphate $(P_nO_{3n+1})^{(n+2)-}$. A 0.02 M aqueous solution of diammonium cerium(IV) nitrate was added dropwise to the phosphoric acid solution (care was taken during the addition to keep the temperature fluctuations to less than 2 °C), and the mixture was allowed to react for 2 h. After washing with water, a flexible, cellulose paperlike material was obtained, suggesting a fibrous morphology.

CeP nanotubes can be synthesized at 105 °C. Although we have not fully clarified the growth mechanism, we believe that the appearance of nanotubes is related to the morphology of the initial condensed linear polyphosphate at the different temperatures. The as-synthesized CeP nanotubes were further heated in a flowing mixture of argon and ammonia (volume ratio of 20:1). A heating rate of 50 $K\,h^{-1}$ was used to allow a smooth structure modification.

The products were analyzed by using an X-ray diffractometer with $Cu_{K\alpha}$ radiation, a differential thermal and thermogravimetric apparatus, a UV/Vis spectrometer, a photoluminescence spectrometer (He-Cd laser, $\lambda_{exc} = 325$ nm), a scanning electron microscope, and a transmission electron microscope (TEM, JEOL 3000F). A Gatan DigiPEELS 766 parallel detection spectrometer attached to the latter microscope was used to collect electron energy loss spectra from an individual nanotube.

Received: July 3, 2004
Published online: December 21, 2004

Keywords: hybrid materials · luminescence · nanostructures · nanotubes · scanning probe microscopy

[1] M. Z. Yates, K. C. Ott, E. R. Birnbaum, T. M. McCleskey, *Angew. Chem.* **2002**, *114*, 494–496; *Angew. Chem. Int. Ed.* **2002**, *41*, 476–478.
[2] a) K. Riwotzki, H. Meyssamy, H. Schnablegger, A. Kornowski, H. Markus, *Angew. Chem.* **2001**, *113*, 574–578; *Angew. Chem. Int. Ed.* **2001**, *40*, 573–576; b) M. Nikl, E. Mihokova, Z. Malkova, A. Vedda, M. Martini, K. Shimmamura, T. Sukuda, *Phys. Rev. B* **2002**, *66*, 184101; c) P. Schlotter, R. Schmidt, J. Schneider, *Appl. Phys. A* **1997**, *64*, 417–418.
[3] R. Francini, U. M. Grassano, L. Landi, A. Scacco, M. D. Elena, M. Nikl, N. Cechova, N. Zema, *Phys. Rev. B* **1997**, *56*, 15109–15114.
[4] a) K. Annapurna, R. N. Dwivedi, P. Kundu, S. Buddhudu, *Mater. Lett.* **2004**, *58*, 7–789; b) Y. X. Pan, M. M. Wu, Q. Su, *Mater. Sci. Eng. B* **2004**, *106*, 251–256.
[5] T. Masui, M. Yamamoto, T. Sakata, H. Mori, G. Adachi, *J. Mater. Chem.* **2000**, *10*, 353–357.
[6] a) S. Iijima, *Nature* **1991**, *354*, 56–58; b) N. G. Chopra, R. J. Cherrey, V. H. Crespi, M. L. Cohen, S. G. Louie, A. Zettl, *Science* **1995**, *269*, 966–967; c) R. Tenne, L. Margulis, M. Genut, G. Hodes, *Nature* **1992**, *360*, 444–446; d) M. Niederberger, H. J. Muhr, F. Krumeich, F. Bieri, D. Gunther, R. Nesper, *Chem. Mater.* **2000**, *12*, 1995–2000; e) P. Hoyer, *Langmuir* **1996**, *12*, 1411–1413; P. Hoyer, *Adv. Mater.* **1996**, *12*, 857; f) C. C. Tang, Y. Bando, Z. W. Liu, D. Golberg, *Chem. Phys. Lett.* **2003**, *376*, 676–682; g) C. N. R. Rao, M. Nath, *Dalton Trans.* **2003**, 1–24.
[7] G. Alberti, U. Constantino, *J. Mol. Catal.* **1984**, *27*, 235–250.
[8] G. Alberti, U. Constantino, F. Di Gregorio, P. Galli, E. Torracca, *J. Inorg. Nucl. Chem.* **1968**, *30*, 295–304.
[9] X. F. Zhang, X. B. Zhang, G. Van Tendeloo, S. Amelinckx, M. Op de Beeck, J. Van Landuyt, *J. Cryst. Growth* **1993**, *130*, 368–382.
[10] J. A. Fortner, E. C. Buck, A. J. G. Ellison, J. K. Bates, *Ultramicroscopy* **1997**, *67*, 77–81.
[11] F. F. Xu, Y. Bando, *J. Appl. Phys.* **2001**, *89*,5469–5472.
[12] A. Fujimori, *Phys. Rev. B* **1983**, *28*, 4489–4493.
[13] a) W. Vanschaik, S. Lizzo, W. Smit, G. Blasse, *J. Electrochem. Soc.* **1993**, *140*, 216–222; b) N. Imanaka, T. Masui, H. Hirai, G. Adachi, *Chem. Mater.* **2003**, *15*, 2289–2291.
[14] E. Nakazawa, F. Shiga, *Jpn. J. Appl. Phys. Part 1* **2003**, *42*, 1642–1647.
[15] N. El Jouhari, C. Parent, G. L. Flem, *J. Solid State Chem.* **1996**, *123*, 398–407.
[16] H. Ebendorff-Heidepriem, D. Ehrt, *Opt. Mater.* **2000**, *15*, 7–25.
[17] A. F. Ali, P. Mustarelli, A. Magistris, *Mater. Res. Bull.* **1998**, *33*, 697–710.

